Investigation of Interfacial Magnetic Properties of Co/C_{60} Hybrid Interface

Mohd Taukeer Khan **Abdullah Almohammedi**

Department of Physics, Faculty of Science, Islamic University of Madinah, Saudi Arabia

Corresponding author,

khanmtk@iu.edu.sa, arda@iu.edu.sa

Abstract: The present work demonstrates a detail investigation of interfacial magnetic properties of cobalt (Co)/fullerene (C_{60}) based ferromagnetic/organic (F/O) hybrid interface. The interfacial structural properties of Co, C_{60} and hybrid interface have been analyzed by X-ray reflectivity (XRR), both computationally and experimentally. The results shows that the grown films have smooth surface (roughness < 0.5 nm) and intermixing at the interface between organic and inorganic layers is less than 1 nm. The spin injection at the hybrid interface was studied by recording the magnetic hysteresis loop at 100 K and photoemission of hybrid interface under the applied bias and magnetic field. It has been observed that due to interfacial spin polarized electron transfer at F/O interface, the photoemission of C_{60} reduces, coercivity of the cobalt increases which give about 18% spin polarization of the carriers injected in C_{60}. Finally, the performance of C_{60} based tunnel junction have been studied in the device configuration viz. Co/Al_2O_3/C_{60}/Py. The magneto resistance (MR) of up to 10 % is obtained for device which having C_{60} layer of thickness 10 nm.

Keywords: Organic spintronics, fullerene, X-ray Reflectivity, magnetoresistance, spin-polarized current

دراسة الخصائص المغناطيسية البينية للواجهة الهجينة Co / C60

الملخص: يوضح العمل الحالي دراسة تفصيلية للخصائص المغناطيسية البينية للكوبالت / (Co) الفوليرين (C60) استنادًا إلى الواجهة الهجينة المغناطيسية / العضوية (ف/ و). لقد تم تحليل الخصائص الهيكلية البينية لـCo ، C60 والواجهة الهجينة بواسطة انعكاس الأشعة السينية (خ ر ر) ، على حد سواء حسابيا وتجريبيا. أظهرت النتائج أن الأفلام المزروعة لها سطح أملس (خشونة <0.5 نانومتر) والتداخل في الواجهة بين الطبقات العضوية وغير العضوية أقل من 1 نانومتر. تمت دراسة الحقن الدوراني في الواجهة الهجينة عن طريق تسجيل حلقة التباطؤ المغناطيسي عند 100 كلفن والإنتاج الضوئي للواجهة الهجينة تحت الجهد المطبق والمجال المغناطيسي. لقد لوحظ أنه نظرًا لنقل الإلكترونات المستقطبة فإن الدوران بين الأقطاب في واجهة ف/ و، يقلل التصوير الضوئي لـ C60 وتزيد قهرية الكوبالت مما يؤدي إلى استقطاب حوالي 18٪ من الناقلات التي تم حقنها في C60. أخيرًا، تمت دراسة أداء تقاطع النفق القائم على C60 في اختبار تكوين الجهاز Co/Al2O3/C60/Py. يتم الحصول على مقاومة مغناطيسية (م ر) تصل إلى 10 ٪ للجهاز الذي يحتوي على طبقة C60 بسمك 10 نانومتر.

1. Introduction

Since past few decades, organic semiconductors (OSCs) have shown auspicious performance in the area of light emitting diodes [1-3], field effect transistors [4-6], photovoltaics [7-11] and spintronics [12-15] due to their small intrinsic size, easy processing, possibility of the fabrication of device in large area, tenability of energy levels according to device requirement. The main attractive aspects of OSCs for spintronics applications is long spin diffusion length (up to 110 nm) due to weak spin-orbit coupling in these materials [16].

Fullerene is very interesting OSCs because it possess numerous properties which make it ideal for organic spintronics devices. Due to absence of hydrogen atom in fullerene, the hyperfine interactions between electron and nuclear spins is very weak and hence reduce the spin-flipping events. Z. G. Yu theoretically predicted that more than 430 nm spin dependent transport length can be achieved for C_{60} at room temperature [17]. It has high electron mobility compare to other OSCs of the order of 1-10 $cm^2/V.s$ [18]. The Fermi levels of commonly used ferromagnetic metals

in spintronic device are quite well matched with lowest unoccupied molecular orbital (LUMO) level of C60 which give rise to a large spin injection from ferromagnetic electrode to C_{60}. Moreover, C_{60} molecules are very robust and sustain the top ferromagnetic electrode without being damage its surface and hence it can be efficiently sandwiched between ferromagnetic electrodes in spin devices [19].

Although there are many advantages for introducing C_{60} molecules in vertical spin device, but there are still many unresolved questions about the working mechanisms of these devices are yet to known. Previously a lot of work has been done to understand the charge transport in organic semiconductors [20-23]. But they have not considered the effect of magnetic field and spin coupling in their studies. The device performance of the OSVs depends upon the reliability of spin injection at F/O interface, spin transport in organic semiconductor and preserving the spin polarized signal. Therefore, the structural and magnetic properties of F/O interface as well as spin transport are the most vital parameters. Henceforth, understanding the structural, magnetic, spin injection and spin polarization and various other spin transport parameters for a spin valve is very vital. The present project aims to study the structural, magnetic properties of Co/C_{60} interface and understand the spin injection, spin transport $Co/C_{60}/Py$ based spin valve.

2. Experimental

The spin valve were fabricated on Si/SiO_2 substrates by using a computerised sputtering system which contains dc magnetron and thermal evaporator in the same chamber. Prior to deposition of thin films, the Si/SiO_2 substrate have been carefully cleaned with propanol then followed by acetone and dried under oxygen flow. The dried substrates were placed inside a sputtering system operated under ultra high vacuum conditions. As a first step tantalum (Ta) seed layer deposited. On top of Ta layer, Co as a bottom ferromagnetic electrode was deposited and then an Al layer was sputtered. To get $A_{l2}O_3$ of desired thickness Al layer was oxidised for optimised time. Fullerene layer was thermally evaporated on top of Co. Finally Permalloy (Py) as a top electrode was deposited. The devices were protected from environmental by depositing a capping layer on top of Py electrode.

3. Results and discussions

3.1 X-ray Reflectivity (XRR)

X-ray reflectivity give the information about the roughness, thicknesses, as well as interfacial mixture of a multilayer film [17]. Figure 1 (a-c) shows the XRR spectra of C_{60}, Co, and [C_{60}/Co]×5 multilayers, respectively. The Kiessig fringes in XRR spectra shown in Fig. 6(a) and (b) extend up to an angle of 3 degrees which confirm the high quality of grown Co and C_{60} surface. The detailed analysis of XRR curves has been performed by using GenX software. GenX is a scientific program to refine XRR using the differential evolution algorithm. The fit to the data for C_{60} shown in Fig. 1 (a) by red line provides the film thickness ~ 26.7 nm, surface roughness σ_{rms} = 5.3 Å and density of layer of 1.6 g/cm^3. The fit to the data for Co shown in fig. 1 (b) by red line give film thickness ~32.4 nm, surface roughness σ_{rms} = 3.4 Å and density of Co of 8.8 g/cm^3.

The XRR spectra of [C_{60}/Co]×5 multilayers is shown in Figure 1 (c). The spectra shows well-defined Kiessig fringes extend up to an angle of 1.5 degrees, intensity decreases uniformly with increase of angle, and well resolved Bragg peak indicates that the bilayer film thickness is uniform through the entire surface. The fit result was obtained by dividing the multilayer in to three layer: C_{60}/Co bilayer/(C_{60}/Co)×3 multilayer/C_{60}/Co bilayer. The fit to the XRR data of the C_{60}/Co multilayers is shown by red line in Fig. 1 (c). From the fitted curves, we obtain the density for the C_{60} layer of 1.63 g/cm^3, and layer thickness of 19.5 nm. The layer thickness of Co in multilayer is found to be 7.8 nm with a density of 8.75 g/cm^3. These results are in good agreement with the expected values. The fitted interface parameters for Co, C_{60} and [C_{60}/Co]×5 multilayer are presented in Table I.

Table 1 Fitting parameters obtained for Co, C_{60} and [C_{60}/Co]×5.

Layer		**Thickness t (Å)**	**Density** d **(g/cc)**	**Surface Roughness σ_{rms} (Å)**	**Interface Roughness (Å)**
C_{60}		265	1.60	5.3	---
Co		324	8.8	3.4	----
[C_{60}/Co]x5	**Co**	78	8.75	5-8	1-2
	C_{60}	195	1.63	8-12	5-9

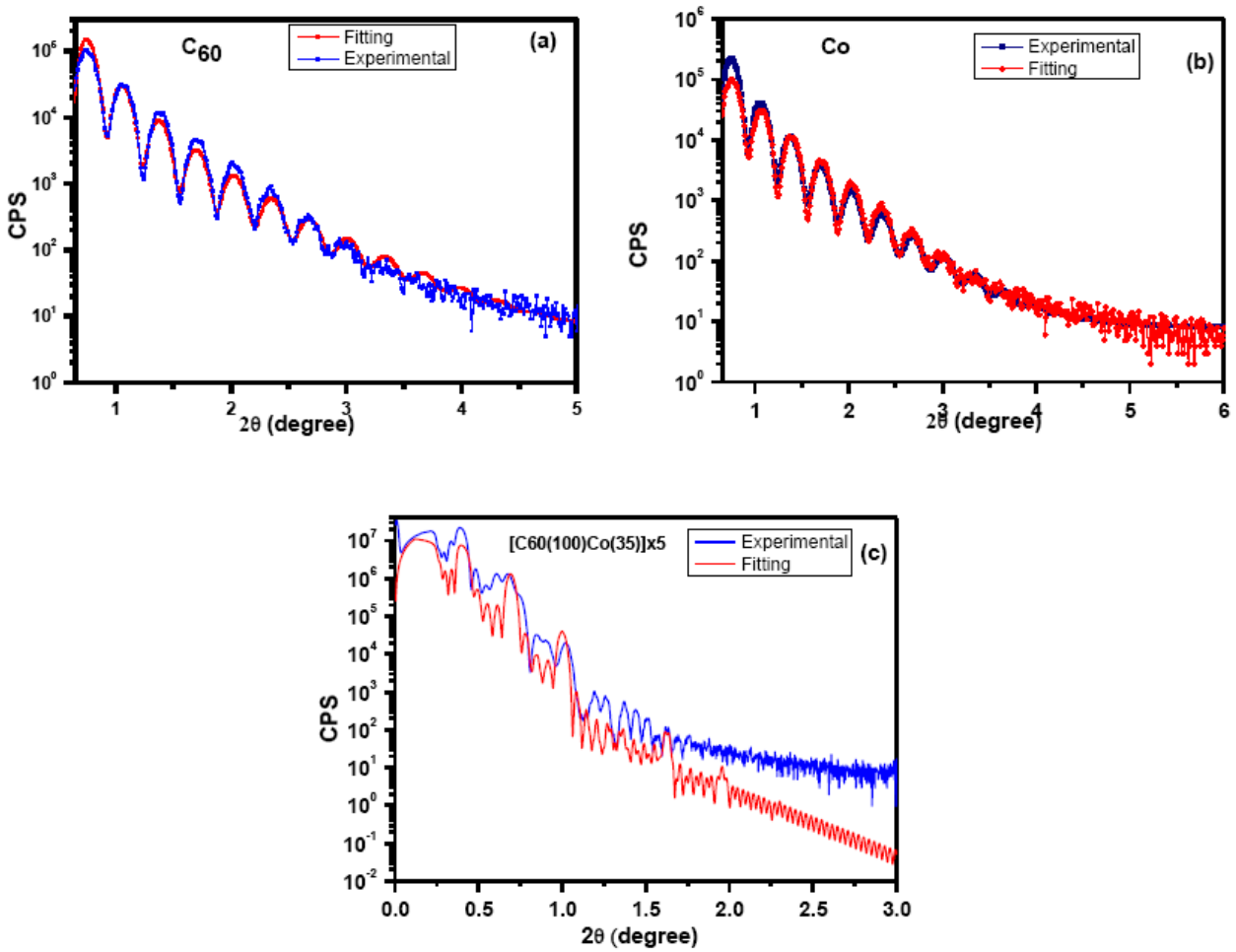

Figure 1: X-ray reflectivity of (a) a C_{60} single layer, (b) a Co single layer, and (c) a [C_{60}/Co]x5 multilayers. Blue lines show the experimental data and red line the fitted line.

3.2 Magnetic Properties of Co/C_{60} Bilayer

After discussing the structural properties of Co and C_{60} layers, our next attention is to analyse the magnetic properties of Co layer when it deposited either above or below the C_{60} layer. For the fabrication of an optimal device, the Co layer must preserve its magnetic properties when it is deposited in a vertical spin device. To understand the effect of molecular layer on the effect of magnetic properties of Co, we have measured the hysteresis loop of different C_{60}/Co and extracted the coercive field (H_c) and the saturation magnetization (M_S).

Figure 2 shows magnetic hysteresis loops, for a 8 nm Co thin film with on top of C_{60} layer with different thickness at 100 K. It has been observed from the Fig. 2 that the M_S value of Co/C_{60} bilayers decreased by 270±10 emu/cc while H_C value increased relative to cobalt layer alone. The

decrease in the value of M_S can be understood as the transfer of spin polarised electron from the Co to the organic. The ferromagnetic properties of Co is due to spin-polarized electron population on 3d band [18]. LUMO of C_{60} molecule is about 4.5 eV and when it comes in contact with the 3d (up) orbital of Co they make a hybridization induced states. When a 20 nm thick C_{60} layer was deposited on top 8 nm Co film, the magnetization of Co layer was reduce about 15%. Moreover increase in H_C value may be result of the local pinning sites caused by surface defects between the organic and the ferromagnet layer [19-21].

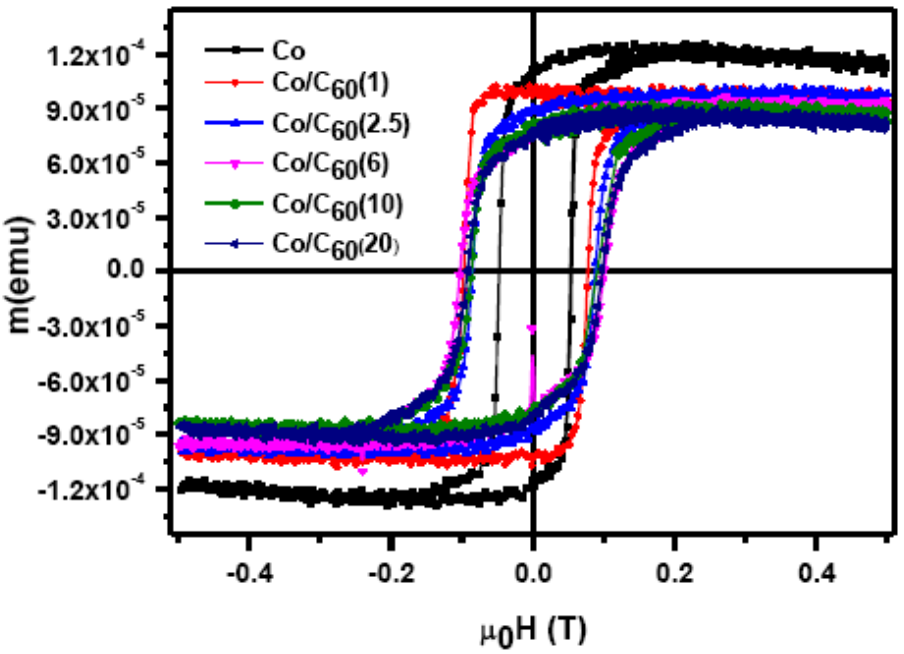

Figure 2: Hysteresis loop of 8 nm Co thin film with on top of C60 layer with different thickness at 100 K. Thickness of C60 are given in bracket.

3.3 Spin-Polarization in C_{60}

To further understand the spin injection from ferromagnet to organic, we have studied the photoemission of C_{60} layer sandwiched between the magnetic electrodes Co and Py. For this purpose we fabricated devices in the configuration viz Ta(5)Co(8)/AlO_x(1.5)/C_{60}(20)/Py(20) (device A) and Ta(5)Co(8)/C_{60}(20)/Py(20) (device B).Under the influence of applied bias charge carrier recombination decreases which results in decrease of photoemission. This is known as negative luminescence (NPL) [22]. Photoemission of device A and device B are shown in Fig. 3(a)

and (b), respectively. When a small current of 1μA/cm^2 and small field of 5 mT was applied across device B, the intensity of photoemission $_0$ remains nearly constant in device B as shown in Figure 3(b). However, in device A when a small current of 1μA/cm^2 was applied, there is drop in the photoluminescence (PL) [Fig. 3(a)]. Furthermore, in device A when a small current of 1μA/cm^2 as well as small field of 5 mT was applied, there is an 18% drop in the PL [Fig. 3(a)].

.

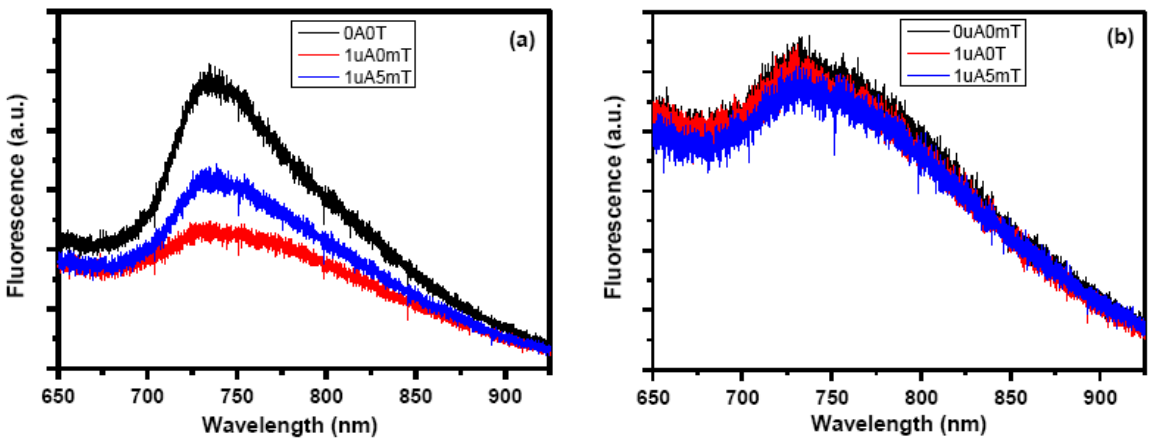

Figure 3: Field dependent florescence spectra of (a)Ta(5)Co(8)/C60(20)/Py(20) (b) Ta(5)Co(8)/AlOx(1.5)/C60(20)/Py(20) excited at wavelength of 532 nm.

This NPL can be understood by the Figure 4. Photoluminescence in organic materials is a spin-dependent phenomenon. As both electron and hole have spins, then according to quantum mechanics, four different combinations of spin are possible: one antiparallel combination of spins, giving a singlet, which emit fluorescence light. On the other hand there are three different combinations of parallel spins are possible, giving a triplet state, and its excitation transferred into heat. When we apply small current in device A, spin polarized electrons are injected by magnetic electrode Co into C60 layer as a results reduction of singlets and increase of triplet electron Figure 4 (b) and hence drops in PL. With the introduction of magnetic field along with current no of singlet electrons further go down and hence PL Figure 4(c). On the other hand when we have Al_2O_3 barrier between FM/Organic interfaces PL is almost constant due to the fact that barrier layer stops the injection of spin polarized electrons from FM electrode to organic layer and hence no of singlet and triplet electrons remains same and hence no NPL.

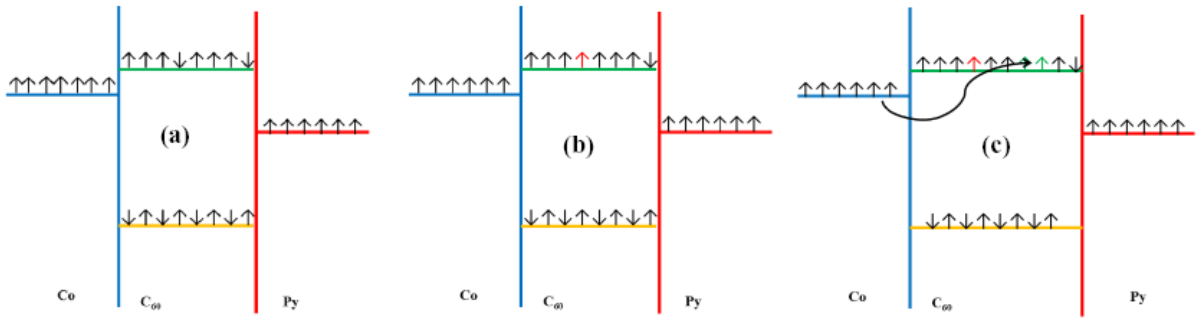

Figure 4: Mechanism of spin transport from Co to C60 in device structure Ta(5)Co(8)/C60(20)/Py(20) (a) without bias and without field (b) 1 μA current and no field (c) 1 μA current and 5 mT field.

3.4 Magnetic Tunnel Junction

We have studied the magneto-transport properties of Co/Al_2O_3/C_{60}/permalloy (Py) multilayer junctions with different thickness of C_{60} layer. C_{60} thickness were taken 0 nm, 10 nm and 20 nm and the corresponding devices are namely, device A, device B and device C, respectively. Due to dissimilar magnetic properties, Py and Co are most common choice of magnetic electrodes for magnetic tunnel junction devices. Py is a nickel–iron magnetic alloy (80% Ni and 20% Fe), with small coercivity (5 Oe for 15-nm thick layer) and high permeability ($\mu=10^5 – 10^6$) while Co is a hard magnetic material with coercivity of about 22 Oe (8 nm thick Co layer) and relatively small permeability. Dissimilar coercivity of Py and Co offers a "window" for changing the orientation of the magnetizations of these two layers, which is a main feature required to achieve the tunnel magneto resistance (TMR).

The fabricated spin valve devices have a cross-bar geometry. These devices were fabricated on Si/SiO_2 (300 nm) substrates by depositing all required layers by sequential deposition inside a sputtering chamber under a high vacuum of ~ 10^{-7} 10^{-8} torr. The final devices configuration of fabricated devices is: Tantalum (Ta, 7.5 nm)/Co(8 nm)/Al_2O_3(1.5nm)/C_{60}(0 or 10 or 20 nm)/Py(15 nm)/Ta(7.5 nm). The Ta layer was deposited on top of Py to prevent the oxidation of it from ambient environment. The Co electrode is used as a spin injector, the spin polarized current is propagated along the organic C_{60} layer and finally detected by the Py electrode. The room temperature resistance as a function of applied magnetic field, at 1 V of fabricated devices (device A, B and C) are displayed in Figure 5 (a-c). The resistance of materials depend on the orientation of net magnetic moment of the electrodes. When both electrodes have parallel configuration of net magnetic moment, the device show low resistance called R_P. On the other hand, when magnetic

electrodes have antiparallel configuration of net magnetic moment, the device shows high resistance R_{AP}. The relative change of resistance is called tunnel magnetoresistance (TMR), is given by equation [23, 24]:

$$TMR = \frac{R_{AP} - R_P}{R_P} \tag{1}$$

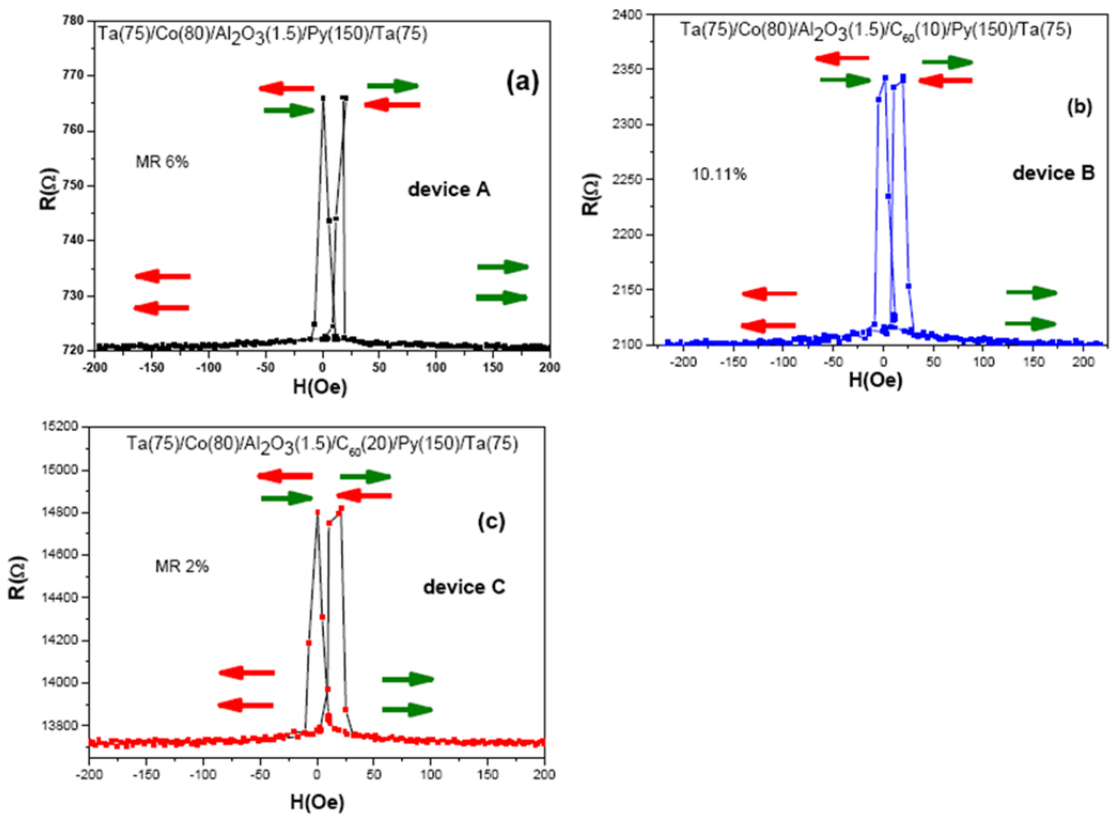

Figure 5 MR measured in (a) device A, (b) device B, and (c) device C.

Figure (5) shows a clear and reproducible TMR, which correspond to the coercive fields of the ferromagnetic layers. For applied field higher than 50 Oe, the two electrodes have parallel configuration of magnetic moments, therefore devices shows low resistance. When magnetic field changes from positive to negative, the magnetic moments of Py switch its orientation due to low coercivity, resulting an antiparallel configuration of magnetic moment and hence devices shows high resistance. When field increases more than 50 Oe in opposite direction, the two electrodes again returns to parallel configuration and device resistance decreases. The reference device A without C_{60} shows MR value about 6%. The maximum MR value of 10.1% is obtained for device B. for device C with the thicker C_{60} (20 nm) layer the MR value goes down 2%. Resistance of

device also depends upon the thickness of organic layer. With the increase of the thickness the resistance of device increases due to the fact of lower mobility in organics.

4. Conclusions

In conclusion, we have successfully analysed the interfacial properties in Co/C_{60} hybrid interface by using multiple structural, photoemission and spin-dependent measurement technique. It has been observed that grown Co, C_{60} and [Co/C_{60}]×5 multilayers have low surface roughness and the intermixing between organic/inorganic interface is less than 1 nm. The coercivity of the cobalt increases when C_{60} is deposited on top of Co which confirm the formation of spin induced hybridization state at F/O interface. With the application of magnetic field and electric current in C_{60} based magnetic device it was found that the photoluminescence of C_{60} was drops by 18%. Finally, the device based on 20 nm thick C_{60} shows >10% of room temperature MR.

5. References

[1] J. Burroughes, C. Jones, and R.H. Friend, New semiconductor device physics in polymer diodes and transistors, Nature, 335 (1988) 137.

[2] J. H. Burroughes, D. D. C. Bradley, A. R. Brown, R. N. Marks, K. Mackay, R. H. Friend, P. L. Burn, and A. B. Holmes. Light-emitting diodes based on conjugated polymers, Nature, 347 (1990) 539.

[3] A. Zampetti A. Minotto F. Cacialli, Near-Infrared (NIR) Organic Light-Emitting Diodes (OLEDs): Challenges and Opportunities, Adv. Funct. Sci., January (2019) https://doi.org/10.1002/adfm.201807623

[4] M. Ahles, A. Hepp, R. Schmechel, and H. V. Seggern, Light emission from a polymer transistor, Appl. Phys. Lett., 84 (2004)428.

[5] L.-L. Chua, J. Zaumseil, J.-F. Chang, E. C.-W. Ou, P. K.-H. Ho, H. Sirringhaus, and R. H. Friend, General observation of n-type field-effect behaviour in organic semiconductors, Nature, 434 (2005)194.

[6] Y. Kim, S. Chung, K. Cho, D. Harkin, W.-Taek Hwang, D. Yoo Jae-Keun, Kim W. Lee Y. Song, H. Ahn, Y. Hong, H. Sirringhaus, K. Kang, T. Lee, Enhanced Charge Injection Properties of Organic Field-Effect Transistor by Molecular Implantation Doping, Adv. Mater., 31, (2019) 1806697.

[7] 17.3% is organic solar cell efficiency record, https://www.electronicsweekly.com/news/research-news/17-3-organic-solar-cell-efficiency-record-2018-08/ .

[8] J. Hou, O. Inganäs, R. H. Friend & F. Gao, Organic solar cells based on non-fullerene acceptors, Nature Materials, 17 (2018) 119–128.

[9] C. Yan, S. Barlow, Z. Wang, H. Yan, A. K.-Y. Jen, S. R. Marder & X. Zhan, Non-fullerene acceptors for organic solar cells, Nature Rev. Mat. 3, (2018) 18003.

[10] M. T. Khan, R. Bhargav, A. Kaur, S.K. Dhawan, S. Chand. Effect of cadmium sulphide quantum dot processing and post thermal annealing on P3HT/PCBM photovoltaic device, Thin Solid Films 519 (2010) 1007.

[11] M. T. Khan, A. Kaur, S K Dhawan and S. Chand, In-Situ growth of cadmium telluride nanocrystals in poly(3-hexylthiophene) matrix for photovoltaic application, J. Appl. Phys 110 (2011) 044509.

[12] Haoliang Liu, Chuang Zhang, Hans Malissa, Matthew Groesbeck, Marzieh Kavand, Ryan McLaughlin, Shirin Jamali, Jingjun Hao, Dali Sun, Royce A. Davidson, Leonard Wojcik, Joel S, Organic-based magnon spintronics. Miller, Christoph Boehme & Z. Valy Vardeny, Nature Materials, 17 (2018) 308–312.

[13] Haoliang Liu, Jingying Wang, Matthew Groesbeck, Xin Pan, Chuang Zhang and Z. Valy Vardeny, Studies of spin related processes in fullerene C_{60} devices, J. Mater. Chem. C, 2018,6, 3621-3627.

[13] Srijani Mallik, Stefan Mattauch, Manas Kumar Dalai, Thomas Brückel & Subhankar Bedanta Effect of magnetic fullerene on magnetization reversal created at the Fe/C60 interface, Scientific Reports, 8 (2018) 5515.

[14] Lidan Guo Xianrong Gu Xiangwei Zhu Xiangnan, Sun Recent Advances in Molecular Spintronics: Multifunctional Spintronic Devices, Adv. Mat. (2019), 1805355, https://doi.org/10.1002/adma.201805355

[15] Shiheng Liang, Rugang Geng, Baishun Yang, Wenbo Zhao, Ram Chandra Subedi, Xiaoguang Li, Xiufeng Han & Tho Duc Nguyen, Curvature-enhanced Spin-orbit Coupling and Spinterface Effect in Fullerene-based Spin Valves, Scientific Reports, 6, (2016) 19461.

[16] Xianmin Zhang, Shigemi Mizukami, Takahide Kubota, Qinli Ma, Mikihiko Oogane, Hiroshi Naganuma, Yasuo Ando & Terunobu Miyazaki, Observation of a large spin-dependent transport length in organic spin valves at room temperature, *Nat. Commun.* 4 (2013) 1392.

[17] Z. G Yu, Spin-orbit coupling and its effects in organic solids, Phys. Rev. B 85 (2012) 115201.

[18] Roderick C. I. MacKenzie, Jarvist M. Frost, and Jenny Nelson, A numerical study of mobility in thin films of fullerene derivatives, J. Chem. Phys. 132 (2010) 064904.

[19] Marco Gobbi Federico Golmar Roger Llopis Fèlix Casanova Luis E. Hueso, Room-Temperature Spin Transport in C60-Based Spin Valves, Adv. Mater. 23 (2011) 1609.

[20] Mohd Taukeer Khan, V. Agrawal, Abdullah Almohammedi, V. Gupta, Effect of Traps on the Charge Transport in Semiconducting Polymer PCDTBT, Solid State Electronics, 145 (2018) 49–53. 4)

[21] Mohd Taukeer Khan, and Abdullah Almohammedi, Effect of CdS nanocrystals on charge transport mechanism in poly(3-hexylthiophene), J. App. Phy., 122 (2017) 075502.

[22] Mohd Taukeer Khan, Amarjeet Kaur, S K Dhawan and Suresh Chand, Hole transport mechanism in organic/inorganic hybrid system based on in-situ grown CdTe nanocrystals in poly(3-hexylthiophene), J. Appl. Phys. 109 (2011) 114509.

[23] Mohd Taukeer Khan, Manisha Bajpai, Amarjeet Kaur, S. K. Dhawan, Suresh Chand, Electrical, optical and hole transport mechanism in thin films of poly(3-octylthiophene-co-3-hexylthiophene): Synthesis and characterization, Synthetic Metals 160 (2010) 1530.

[24] Elements of Modern X-ray Physics, by J. Als-Nielsen and Des McMorrow, 2nd Edition wiley, (2001).

[25] Handbook of Thin Film Materials: Nanomaterials and Magnetic Thin Films by H. S. Nalwa, Academic Press, (2002).

[26] Y.-L. Chan, Y.-J. Hung, C.-H. Wang, Y.-C. Lin, C.-Y. Chiu, Y.-L. Lai, H.-T. Chang, C.-H. Lee, Y. J. Hsu, and D. H. Wei, Magnetic Response of an Ultrathin Cobalt Film in Contact with an Organic Pentacene Layer, Physical Review Letters 104 (2010) 177204.

[27] A. A. Sidorenko, C. Pernechele, P. Lupo, M. Ghidini, M. Solzi, R. De Renzi, I. Bergenti, P. Graziosi, V. Dediu, L. Hueso, and a. T. Hindmarch, Interface effects on an ultrathin Co film in multilayers based on the organic semiconductor Alq_3, App. Phy. Let. 97 (2010) 162509.

[28] I. Bergenti, a. Riminucci, E. Arisi, M. Murgia, M. Cavallini, M. Solzi, F. Casoli, and V.

Dediu, Magnetic properties of Cobalt thin films deposited on soft organic layers, Journal of Magnetism and Magnetic Materials 316 (2007) e987.

[29] Y-J., L.Y.-L. Hsu, C-H. Chen, Y-H. Lin, H-Y. Chien, J-H.Wang, T-N. Lam, Y-L. Chan, D. H. Wei, H-J. Lin and C-T. Chen, Self-Assembled Graphene/Carbon Nanotube Hybrid Films for Supercapacitors, The J. Phy. Chem. Lett., 4 (2012) 310.

[30] J. S. Moodera and G. Mathon, Spin polarized tunneling in ferromagnetic junctions, J. Magn. Magn. Mater., 200 (1999) 248–273.

[31] M. Julliµere, Tunneling between ferromagnetic films, Phys. Lett. 54, (1975) 225.